

Article

Prediction and Surface Roughness Optimization in Die-Sinking EDM of AA 5083 Using RSM and Swarm Intelligence Algorithms

Nikolaos A. Fountas and Nikolaos M. Vaxevanidis *

Laboratory of Manufacturing Processes & Machine Tools (LMProMaT), Department of Mechanical Engineering Educators, School of Pedagogical and Technological Education (ASPETE), 151 22 Amarousion, Greece

* Correspondence: vaxev@aspete.gr**How To Cite:** Fountas, N.A.; Vaxevanidis, N.M. Prediction and Surface Roughness Optimization in Die-Sinking EDM of AA 5083 Using RSM and Swarm Intelligence Algorithms. *Bulletin of Computational Intelligence* 2026, 2(1), 1–12. <https://doi.org/10.53941/bci.2026.100001>

Received: 14 August 2025

Revised: 7 October 2025

Accepted: 30 October 2025

Published: 5 January 2026

Abstract: As a non-conventional thermal material removal process, electro-discharge machining (EDM) is preferred when it comes to complex features and with high-precision contours as well as for materials that cannot be processed via conventional material removal operations. Nevertheless, several phenomena may adversely affect surface integrity of EDMed components, thus; they should be considered and experimentally investigated to optimize electro-discharge machining process. This paper experimentally examines surface integrity as regards surface roughness average Ra when using AA 5083 as a workpiece material and copper as electrode. Experiments were designed and carried out according to Taguchi L₉ orthogonal design, setting three different levels of the process control parameters namely discharge (peak) current, pulse-on time and pulse-off time. Three algorithms namely moth-flame algorithm, dragonfly algorithm and whale optimization algorithm were employed to minimize the response. All algorithms performed adequately; however obvious differences in convergence speed and optimal solution results were found. The lowest result for surface roughness was found equal to 4.410 μm by DA and WOA algorithms at 35th and 5th iterations respectively, whereas DA was converged to its lowest score equal to 4.736 μm after 35 iterations

Keywords: electro-discharge machining; surface roughness; AA 5083; response surface methodology; swarm intelligence

1. Introduction

Die-sinking electrical discharge machining (EDM) constitutes one of the most widely-employed non-conventional material removal processes with emphasis to the production of complex contours, profiles and patterns. In addition die-sinking EDM process is mainly preferred for the machining of hard engineering materials accompanied with high-quality specifications involving tight tolerances and dimensional accuracy [1]. Die-sinking EDM technology suggests both the tool-electrode and workpiece to be fully immersed in a container (machine working cabin) with dielectric fluid while applying discharge pulses between them to achieve non-contact sequential erosions (spark discharges) and thus material removal by local melting and/or workpiece material evaporation. The resulting eroded surface is characterized by overlapping craters and features indicative of the intense thermal phenomena involved [2–5]. To ensure stability of die-sinking EDM process a servo-controlled apparatus usually integrates the die-sinking EDM system. The final result is the tool's-electrode's complementary shape impression on the workpiece surface having a predetermined “over-cut” to be left for finish-machining using conventional material removal processes; i.e., milling.



The operational principles of die-sinking EDM obviously adhere to a complex thermal material-removal mechanism that involves plasma channel formation between electrode and workpiece melting and evaporation phenomena as well as shock waves. Consequently machined materials are imposed to metallurgical transformations that involve phase changes, residual stresses and cracks. Among other important attributes related to EDM machinability, the aforementioned aspects are all expressed by the term “surface integrity” and specify the operational behavior of EDMed components [1,2].

Despite that material removal processes are nowadays well-established for their usage to industrial production; an on-going research is notable dealing with EDM process modeling [6,7], EDM parameter effects investigation [8–13] and process optimization with machine learning, genetic/evolutionary algorithms and general computational intelligence [14–17]. A successful application of a manufacturing process such as EDM depends on achieving reliable (if not optimal) performance in terms of a number crucial metrics such as material removal rate, tool wear rate (such as the electrode in the case of EDM) and final surface finish exhibited by surface roughness indicators. Undoubtedly EDM exhibits low material removal rates since it is mainly dedicated to finishing phases. Therefore it is crucial to reduce the overall cost by optimizing the final surface finish and avoid further post-processing operations.

Major scope of the study is to demonstrate the efficiency of a selected number of swarm-based evolutionary algorithms namely moth-flame optimization algorithm (MFO) [18], the dragonfly algorithm (DA) [19] and the wale optimization algorithm (WOA) [20] in terms of global best result quality and convergence speed when applied to solve actual material removal constrained optimization problems with emphasis to die-sinking EDM and its resulting surface integrity outcomes with reference to surface roughness average, R_a (μm). It should be noted that these algorithms as well as others that fall to swarm intelligence and bio-inspired computation [21] and are yet to be applied to manufacturing optimization problems and especially in non-conventional material removal processes such as EDM [22–25]. Therefore their application for optimizing the problem presented in this paper constitutes the main contribution and novel aspect that distinguishes this research among notable others related to manufacturing process optimization.

2. Materials and Methods

2.1. Design of Experiments

Among the several approaches provided for establishing systematic experimental designs, the L_9 Taguchi orthogonal array (OA) was selected to reduce experimental runs and cost as regards resources and equipment usage. Among the crucial EDM-related independent parameters affecting surface roughness, three of them were selected; namely discharge current I_p (A), pulse-on time T_{ON} (μs) and pulse-off time T_{OFF} (μs) since they are considered of paramount importance [3–5,11]. The independent EDM-related parameters for assessing surface roughness R_a (μm); discharge current I_p (A), pulse-on time T_{ON} (μs) and pulse-off time T_{OFF} (μs) as well as their experimental levels, are shown in Table 1.

Table 1. Design of EDM experiments according to L_9 orthogonal array.

EDM Parameter	Symbol	Level			Unit
		1	2	3	
Discharge current	I_p	6	9	15	(A)
Pulse-on time	T_{ON}	75	150	300	(μs)
Pulse-off time	T_{OFF}	50	100	150	(μs)

Among the several roughness parameters, the arithmetic surface roughness average-or simply mean surface roughness, R_a (μm)-was chosen as the response of major interest owing to its wide employment as a surface integrity indicator referring to academic/engineering research branches and industrial applications.

2.2. EDM Experimental Setup and Measuring Equipment

EDM experiments according to the L_9 Taguchi orthogonal array design were conducted in an ONA[®] QX3F die-sinking CNC electro-discharge machine equipped with fixed-bed plate allowing long travel length on X, Y and Z axes with high stability. Prior to the experiments, standard CNC operations related to home point set and G-code coordinates corresponding to each of the 9 EDM electrode positions were programmed. These operations were conducted using the closed-loop CNC controller that integrates the machine’s EDM control system. Nine trials were sequentially conducted based on the G-code program developed whereas the nine resulting erosions were measured using a TESA[®] Rugosurf[®] 10 G portable roughness tester. For the measuring tests a cut-off length

l_c equal to 0.8 mm was set as per the ISO 4287 standard. Each EDMed cylindrical region was measured three times using the software environment (Rugosoft 10G[®], Version: 1.5.1.026) accompanying the roughness tester and the mean result of these three independent measurements was considered to represent the obtained roughness. The overall machining apparatus and measuring equipment are depicted in Figure 1a,b respectively.



Figure 1. EDM experimental setup and roughness measurements: (a) EDM machining setup; (b) Roughness measurements and corresponding measurement processing environment.

2.3. Workpiece Material, Electrode Tool and Dielectric Fluid

A rectangular AA 5083 block of 100 × 100 mm with 30 mm thickness was selected as the work piece material for EDM machining tests. This aluminum alloy was selected for its exceptional performance in extreme environments; considered as highly resistant to industrial chemical environments. The chemical composition and the properties of AA 5083 alloy are summarized in Tables 2 and 3 respectively whereas Figure 2 illustrates the AA 5083 work piece block used.

Table 2. Chemical composition of AA 5083 alloy.

Element	Al	Si	Fe	Cu	Mn	Mg	Zn	Ti	Cr
% content	92.4–95.6	0.4	0.4	0.1	0.4–1.0	4.0–4.9	0.25	0.15	0.05–0.25

Table 3. Properties of AA 5083 alloy.

AA 5083 Properties	Range
Proof Stress	125 MPa
Tensile Strength	275–350 MPa
Hardness Brinell	75 HB
Density	2650 kg/m ³
Melting Point	570 °C
Modulus of Elasticity	72 GPa
Electrical Resistivity	$0.58 \times 10^{-6} \Omega \cdot m$
Thermal Conductivity	121 W/m.K
Thermal Expansion	$25 \times 10^{-6}/K$

As a working tool (electrode) an electrolytic copper material was selected. The electrode was cut using a mechanical saw and then finish-machined using a conventional lathe. The cylindrical electrode was $\Phi 20$ mm in its operational diameter and 70 mm in overall length (Figure 3a). The tool was suitably machined to be safely clamped to the machine's Z-axis carrying the electrode as Figure 3b depicts. The specific electrode material type was preferred owing to its high electrical conductivity and its known general properties that facilitate such non-conventional material removal operations like die-sinking EDM processes (Figure 3c).

Fuchs[®] EcoSpark[®] 105 was used as the dielectric solvent for the experiments. The specific type of dielectric is an odourless and colourless paraffinic solvent that exhibits excellent cooling and flushing properties owing to its low viscosity (3.3 mm²/s at 20 °C) and high flash point above 100 °C. In addition the excellent filterability

concerning both wire and die-sinking EDM enables the efficient sparking operation accompanying with relatively high material removal rates with low electrode wear.

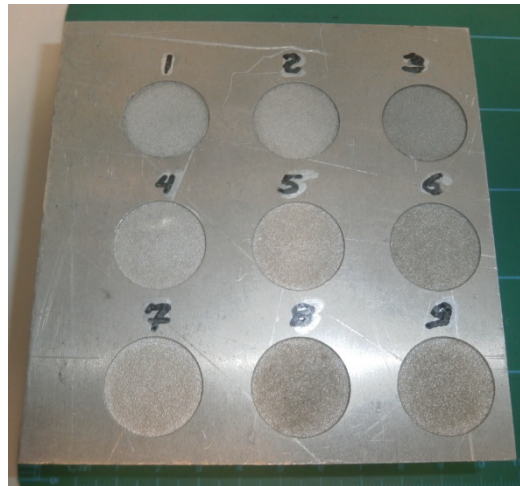


Figure 2. Rectangular block of AA 5083 alloy used for EDM experiments.

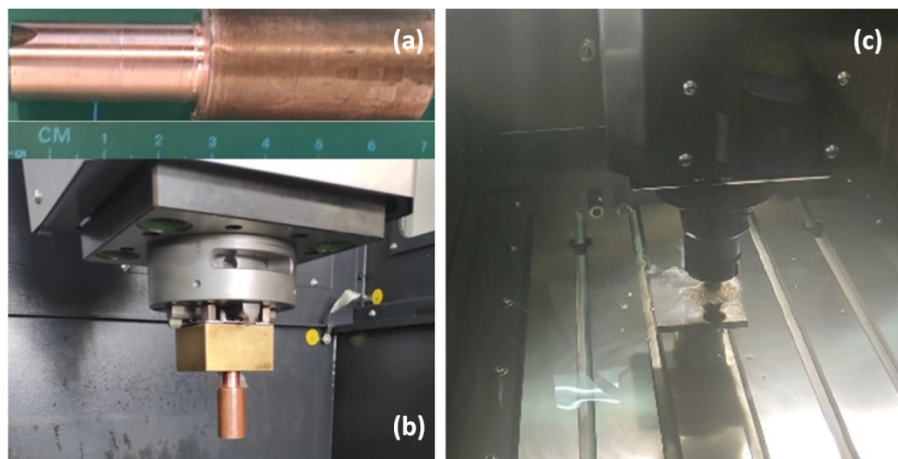


Figure 3. Working tool and setup: (a) Electrolytic copper tool-electrode (anode); (b) The ONA QX 3F electrode (tool) holder (c) Indicative preliminary experimental EDM operation on a 10 mm thick 5083 alloy.

2.4. Swarm Intelligence Algorithms

Swarm-intelligent based algorithms that simulate the social behavior of natural species and have already implemented in almost every scientific field related to engineering, manufacturing and general industrial problem-solving applications [21]. Notable metaheuristics of this category that have been recently developed and applied to several areas of engineering science are the moth-flame optimization algorithm (MFO) [18], the dragonfly algorithm (DA) [19] and the whale optimization algorithm (WOA) [20] among others. However these algorithms are yet to be implemented to optimization problems related to manufacturing technology with emphasis to non-conventional material removal processes. These algorithms exhibit different operational behavior whereas each of them simulates a major physical aspect of different living species that are considered as the “search agents” (candidate solutions). Moth-flame optimization algorithm (MFO) establishes and implements artificial moths as its search agents-candidate solutions. As a result the positions of hypothetical moths in the search domain are assumed to be the problem’s independent variables. Based on the problem’s characteristics these positions are iteratively updated until the algorithm concludes the predetermined simulations. “Flames” represent the beneficial positions found by moths corresponding to each evaluation. In addition the “flames” are assumed as flags or pins that moths drop as long as a solution domain is searched. Thereby moths examine the flags and update them if a better solution than the current one has been found, hence; facilitating the best solution preservation concept. A random population of moths is first created and then moths are moved towards the search domain. As the optimization process evolves, positions of moths are updated with regard to flames. Updating process referring to moths and flames facilitates exploitation mechanism of the algorithm; however a logarithmic spiral-type path should be programmed to maintain the major update operator. Further attributes concerning the MFO algorithm

including the aforementioned aspects, can be found in [18]. Dragonfly algorithm's (DA) operation mimics the natural concept of dragonflies as predators, towards the hunting and capturing all other smaller insects found in the environment. Owing to the needs for both hunting and migration, natural dragonflies present unique swarming characteristics. "Hunting" operator suggests the algorithm's static behavior simulation, whilst "migration" operator suggests the algorithm's dynamic behavior. The aforementioned mechanisms correspond to the algorithm's local search with the aid of dragonflies' static swarm divided to small groups and the search process of restricted regions in the solution domain. There is also a probability of small dragonfly swarms to abruptly change their path towards a "back-and-forth" trajectories style. Dynamic dragonfly swarms are indicated to migrate to a long-distance direction. Even though there is an obvious difference comparing these two swarm behaviors, notable similarities are found as regards exploration and exploitation phases. The several regions of the search space that are visited by static dragonfly sub-swarms introduce the exploration process simulated by DA. On the other hand, if a specific direction is to be visited by larger dragonfly sub-swarms, then exploitation process is facilitated. Consequently, a variety of different strategies corresponding to exploration and exploitation mechanisms may be simulated by properly determining the algorithm's operation-related parameters for problem-solving. Further attributes concerning the DA algorithm including the aforementioned aspects mentioned, can be found in [19]. The Whale Optimization Algorithm (WOA) is a meta-heuristic optimization algorithm [20] inspired by the hunting behavior of humpback whales. It is used to solve complex optimization problems by simulating three key stages: encircling prey, "bubble-net" attacking (exploitation), and searching for prey (exploration). WOA implements a population of search agents (whales) and seeks to find the best solution in a given search space. The three major mechanisms that WOA employs to solve an optimization problem are "prey encircling", "bubble-net attack" and "shrink-wrap". Whales identify the best location (optimal solution) and surround it. Bubble-Net attack simulates exploitation phase where a spiral-type path of bubbles is created. Whales move in this spiral path towards the best solution to update their positions (shrink-wrap). Mathematical modeling of this mechanism involves a decreasing coefficient that controls the path trajectory. Algorithmic features of Whale optimization algorithm (WOA) are given in [20].

3. Results and Discussion

3.1. Experimental Results, ANOVA Analysis and Parameter Effects

Die-sinking EDM experiments were sequentially performed according to the design of experiments established. Table 4 summarizes the results concerning surface roughness average according to the parameter levels based on the design of experiments according to the L₉ OA design.

Table 4. Experimental results for mean surface roughness R_a , (μm) based on L₉ orthogonal array DoE.

No. Exp.	Discharge Current, I_P (A)	Pulse-on Time, T_{ON} (μs)	Pulse-off Time, T_{OFF} (μs)	R_a (μm)
1	6	75	50	4.860
2	6	150	100	4.400
3	6	300	150	5.392
4	9	75	100	5.935
5	9	150	150	8.137
6	9	300	50	8.204
7	15	75	150	9.452
8	15	150	50	11.760
9	15	300	100	12.229

According to the results the 2nd experiment found the most beneficial with reference to its surface roughness average result that was the lowest; i.e., 4.40 μm . To further examine the results in terms of EDM process parameter effects as well as to establish reliable regression models, the initial L₉ orthogonal array design of experiments was turned to a custom response surface design. This enabled the examination of interactions and the generation of full quadratic regression models based on the "least squares" regression modeling approach. Both hierarchy and significance of EDM process parameters on the response of surface roughness average are studied through ANOVA (Table 5) whereas the regression model comprising the significant terms is given in Equation (1).

$$R_a = -1.02 + 0.742 \times I_P + 0.0004 \times T_{ON} + 0.0278 \times T_{OFF} + 0.00093 \times I_P \times T_{ON} - 0.00238 \times I_P \times T_{OFF} - 0.000039 \times T_{ON} \times T_{OFF} \quad (1)$$

Based on the results presented in Table 5 it can be observed that discharge current and pulse-on time are the two most influential process parameters followed by the interaction effects among discharge current with pulse-

on time and discharge current with pulse-off time. This justifies the elimination of other model terms in order to maintain high model accuracy indicators. Note that discharge current is deemed as crucial process-related parameter to EDM operations since it increases discharge energy, thus; leading to large overlapping craters formulated by molten and evaporated material, micro-cracks and increased porosity on part's surface.

The results indicate that the regression model developed for predicting surface roughness average exhibits a high correlation degree ($R^2 = 96.22\%$). Both R^2 and R^2 (adj.) values corresponding to the regression model are greater than or quite close to 85% respectively. In addition the difference between the two indicators is less than 20%. These outputs suggest strong evidence that the model presents high correlation between EDM-related process parameters and average surface roughness, proving its feasibility and adequacy. Figure 4 depicts the interaction effects found among the most influential EDM process parameters; that of discharge current vs. pulse-on time $I_P \times T_{ON}$ (Figure 4a) and discharge current vs. pulse-off time $I_P \times T_{OFF}$ (Figure 4b).

Table 5. ANOVA table for response surface regression: Ra (μm) vs. I_P , T_{ON} , T_{OFF} .

Source	DF	Seq. SS	Adj. SS	p-Value
Model	6	65.0457	65.0457	-
Linear	3	64.0232	46.2369	-
I_P (A)	1	58.9731	44.2145	0.028
T_{ON} (μs)	1	4.4654	2.3809	0.031
T_{OFF} (μs)	1	0.5847	0.2350	0.071
2-way int.	3	1.0225	1.0225	-
$I_P \times T_{ON}$	1	0.3611	0.6510	0.055
$I_P \times T_{OFF}$	1	0.5548	0.6430	0.055
$T_{ON} \times T_{OFF}$	1	0.1067	0.1067	0.080
Error	2	2.5582	2.5582	-
Total	8	67.6039	-	-
R^2	96.22%			-
R^2 (adj.)	84.86%			-

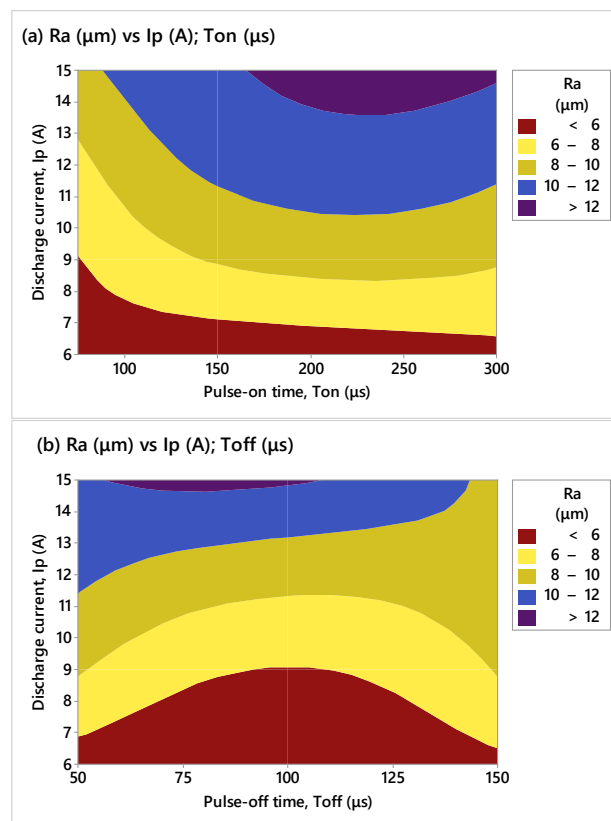


Figure 4. Contour plots for interaction effects on Ra : (a) Ra vs. $I_P \times T_{ON}$; (b) Ra vs. $I_P \times T_{OFF}$.

A residual analysis conducted to further question the adequacy of the regression model in terms of its robustness and reliability. The normal probability of residuals was examined with respect to its resultant p-value equal to 0.924.

This result is far beyond the confidence level's value of 0.05; therefore the regression model is reliable and adequate for further employment either as a correlation entity between inputs and outputs or as an objective function for repetitively evaluating fitness scores provided by intelligent algorithms, aiming at minimizing surface roughness. Figure 5 depicts the probability plot of the model's residuals at 95% confidence level.

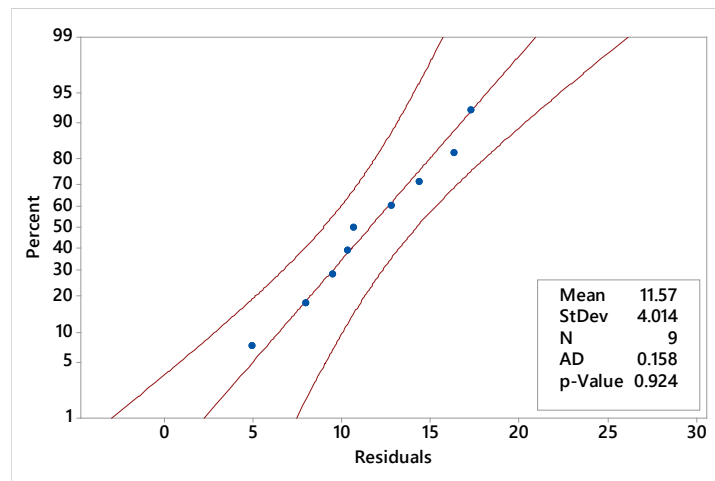


Figure 5. Probability plot of residuals at 95% confidence level. The blue dots in the figure represent the residuals obtained by the statistical analysis conducted (at 95% confidence level) to generate out regression models.

3.2. Surface Roughness Optimization Using Swarm Intelligence Algorithms for EDM

The regression model developed for predicting the response of surface roughness average was used as an objective function to be iteratively evaluated by the three algorithms presented. Algorithmic simulations for the algorithms were conducted under equal terms and conditions to provide rigorous comparative analysis concerning the best (minimum) result for average surface roughness Ra (μm) and convergence speed along with the algorithms' capability of avoiding local trapping. Note that an algorithm's convergence curve reveals how its performance is improved over iterations. Steeper curves present faster convergence towards the optimal solution. The solution domain was constrained to the same range (low-high levels) for independent EDM process parameters whereas each candidate solution is represented by a vector referring to the values of the three EDM parameters within their predefined bounds. For the problem under examination, algorithm-related parameters were determined mainly with emphasis to computational cost and time-pressing industrial requirements. Therefore the number of iterations was intentionally restricted to 100 whilst the number of search agents (candidate solutions, i.e., moths, dragonflies and whales) were set equal to only 5. Simulations were run in MATLAB[®] 2014b. The single-objective optimization problem formulated according the response of surface roughness Ra and the experimental range of the selected EDM process parameters, is mathematically described as follows (Equation (2)):

$$\min Ra (I_P, T_{ON}, T_{OFF}) \quad (2)$$

subjected to the bounds according to Equations (2)–(5).

$$I_P \min = 6 \text{ A} \leq I_P \leq I_P \max = 15 \text{ A} \quad (3)$$

$$T_{ON} \min = 75 \mu\text{s} \leq T_{ON} \leq T_{ON} \max = 300 \mu\text{s} \quad (4)$$

$$T_{OFF} \min = 50 \mu\text{s} \leq T_{OFF} \leq T_{OFF} \max = 150 \mu\text{s} \quad (5)$$

The algorithms tested, needed less than 8 s to converge to the final recommended optimal solution. Simulations were conducted in an Intel[®] core[™] i3-4160 CPU 3.60 GHz 8GB RAM 64 bit operating system. Figure 6 illustrates the convergence curves obtained by MFO (Figure 6a); DA (Figure 6b) and WOA (Figure 6c) whereas Figure 6d gives a comparative depiction among the three convergence curves of algorithms to allow for their simultaneous assessment. Note that these results correspond to a single independent run.

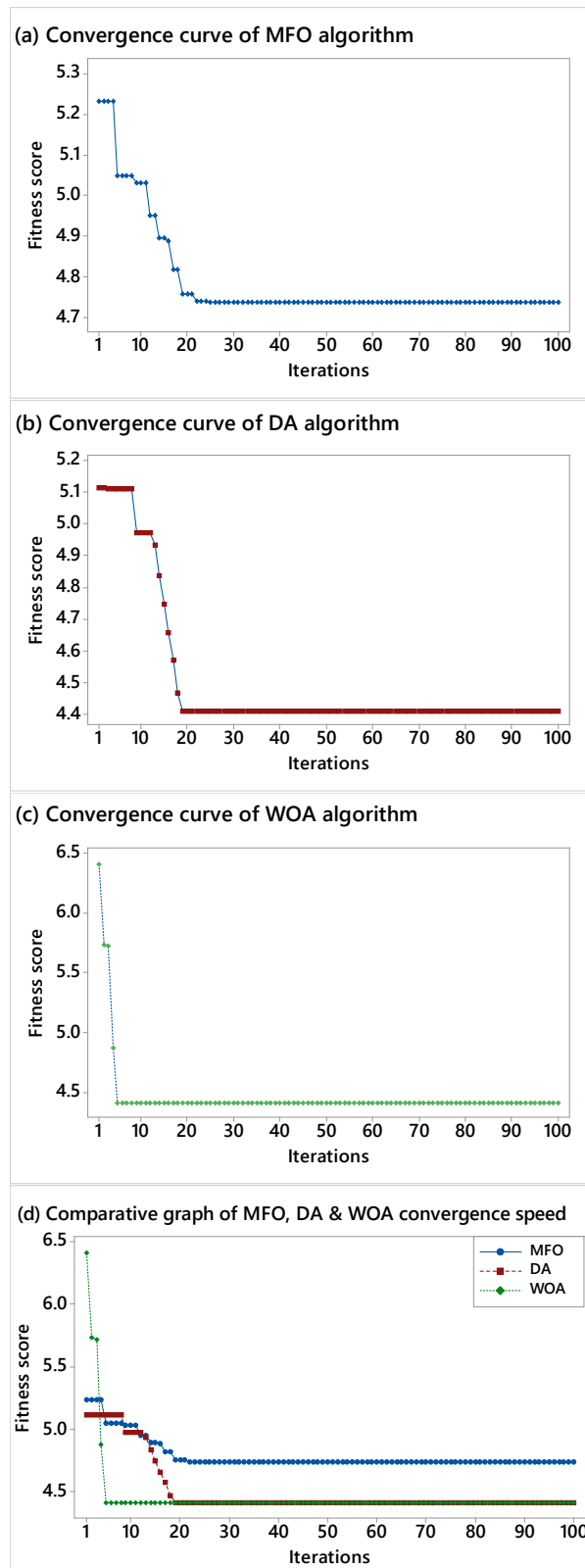


Figure 6. Convergence graphs obtained by swarm-based intelligent algorithms: (a) MFO; (b) DA; (c) WOA; (d) comparative graph of all algorithms.

It is observed that the algorithms tested, not only arrive in different global optima but also exhibit different operational behavior in terms of converge speed and local trapping avoidance. By examining Figure 6a referring to MFO algorithm, evaluations start by finding a value equal to 5.233 μm for Ra at an early stage whereas the final result suggests 4.736 μm . The global minimum value was obtained in 30th iteration with MFO algorithm to escape from local optimal values approximately seven times. As regards the EDM process-related parameter settings, the global optimum (minimum) result for surface roughness average comes with 6 A for discharge current, 155.8 μs

for pulse-on time and 50 μs for pulse-off time. DA algorithm started by reaching the value equal to 5.115 μm whereas the minimum result was found equal to 4.410 μm at 19th iteration. This result suggests 6 A for discharge current, 75 μs for pulse-on time and 50 μs for pulse-off time in terms of EDM parameter settings. DA algorithm experienced local trapping approximately two-to-three times based on its convergence curve (Figure 6b); however it managed to rapidly escape towards finding its global optimum result for surface roughness average. Finally WOA algorithm obtained its lowest fitness score in 5th iteration, equal to 4.410 μm whilst it started its evaluation scores with a value equal to 6.406 μm which was the highest one compared to those obtained by MFO and DA algorithms (Figure 6c). Its lowest (optimal) result is achievable by setting 6 A discharge current, 75 μs pulse-on time and 50 μs pulse-off time as in the case of DA algorithm. Algorithmic evaluations were conducted in less than 5 s, referring to all three algorithms; MFO, DA and WOA. To assess reliability of the algorithms tested, a set of ten independent simulations were conducted to evaluate their average performance. Figures 7–9 illustrate the results obtained by MFO, DA and WOA algorithm respectively, revealing WOA algorithm's superiority in terms of variance, standard deviation and simulation error.

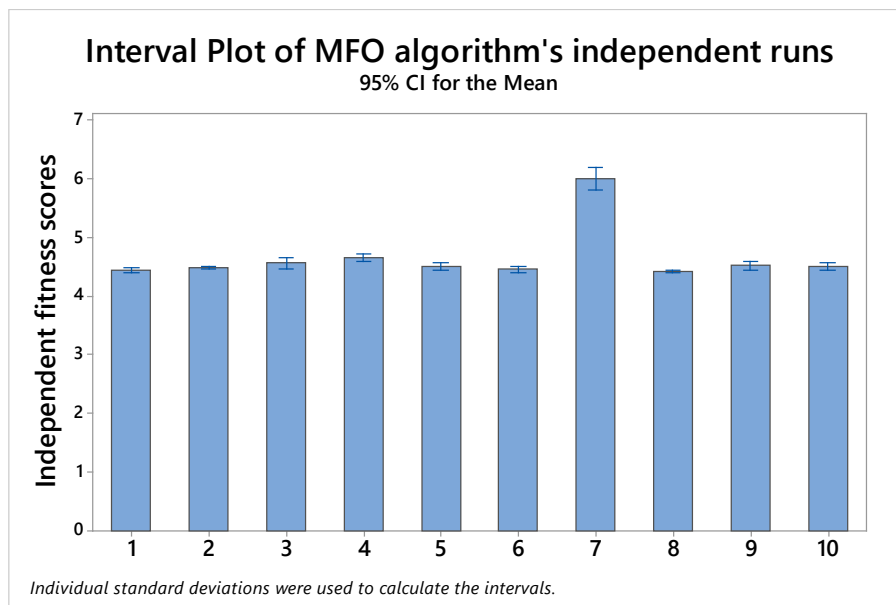


Figure 7. Independent fitness scores for evaluating MFO algorithm.

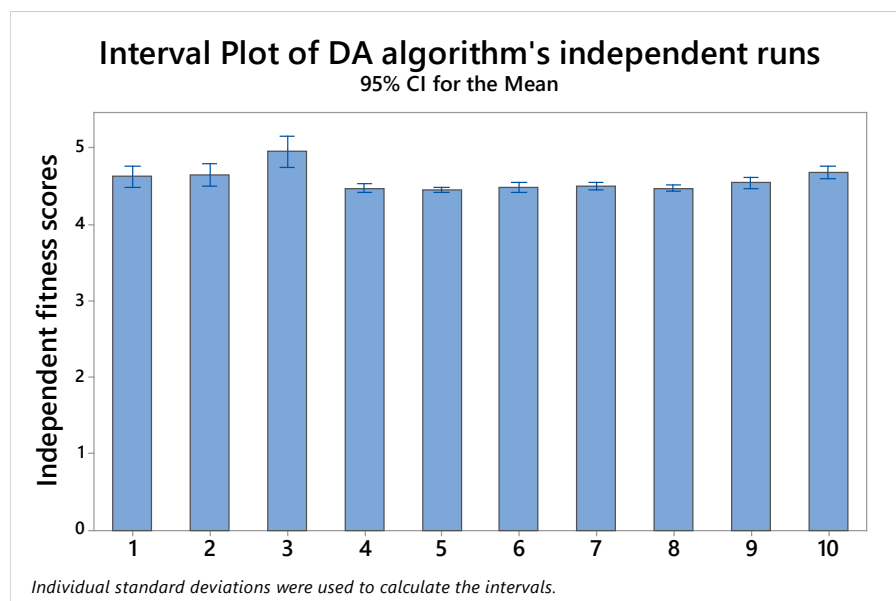


Figure 8. Independent fitness scores for evaluating DA algorithm.

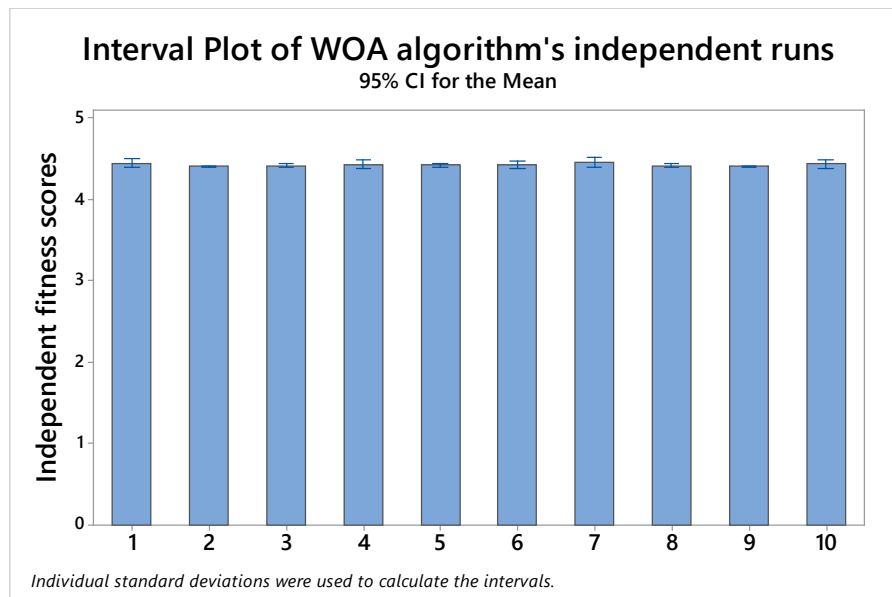


Figure 9. Independent fitness scores for evaluating WOA algorithm.

4. Conclusions

In this study the functional relationship among three important die-sinking EDM parameters concerning the AA 5083 aluminum alloy having copper electrode for successive erosions, have been examined for their effect on the response of surface roughness average, Ra (μm). The parameters under study where the discharge (peak) current, (A); pulse-on time, TON (μs) and pulse-off time, $TOFF$ (μs). A Taguchi L_9 orthogonal array design of experiments was established to prepare the experimental protocol and conduct die-sinking EDM experiments to obtain the results necessary for further investigation and statistical analysis. The outcome from the analysis was a regression equation with high correlation capability and good predictability of the response of surface roughness average. The regression model generated was further employed as the objective function for minimizing the response of surface roughness average, by implementing three intelligent algorithms; the moth-flame optimization algorithm (MFO); the dragonfly algorithm (DA) and the whale optimization algorithm (WOA). The research effort was conducted because die-sinking EDM is a complex non-conventional thermal material-removal process and therefore is rather difficult to obtain good functional relationship among independent parameters and one -or more than one-objectives. From a practical perspective such an approach is low-cost and easy to implement while it offers viable and reasonable outputs for industrial purposes. As general conclusions the following observations are notable:

- All algorithms perform adequately fast in terms of their task towards finding the optimal solution; either minimum or maximum depending on the problem. However their intelligent operators suggest different perspectives of efficiency and reliability despite the problem's common solution domain representation; i.e., a full quadratic regression model.
- By observing the convergence evolution of the algorithms tested, it is observed that local stagnations occur from where all algorithms rapidly manage to avoid. This justifies their well-established operational behavior and robustness on solving optimization problems at least when it comes to non-conventional material removal processes like EDM. However notable differentiations related to the algorithms' performance and operational behavior suggest the clear superiority of WOA algorithm against MFO and DA. Referring to WOA the final result obtained by a single run for minimizing Ra was found equal to $4.410 \mu\text{m}$. In addition WOA exhibited the lowest variation, lowest standard deviation and stable average performance when comparing fitness score samples obtained by performing multiple evaluation runs. WOA's operational behavior suggests also a broader solution space assessment since its starting fitness score at early stages reaches the largest value compared to those presented by MFO and DA algorithms.
- The results obtained by the different algorithms are undoubtedly of minor difference when examined from the perspective of their arithmetic values. Nevertheless quality restrictions, process requirements and manufacturing costs should be the factors that decision makers should take into account to implement an intelligent algorithm for solving manufacturing problems related to production tasks.

Looking further ahead, the authors are to extend the research to other responses such as material removal rate, electrode wear as well as the usage of other population and/or swarm-based computational variants to test

and compare efficiency and applicability to conventional/non-conventional material removal technologies such as die-sinking EDM, wire EDM, etc. In addition more experiments will be performed for investigating the effect of die-sinking EDM input variables on a variety of engineering materials.

Author Contributions

N.A.F. & N.M.V.: Conceptualization, methodology, software; N.A.F.: Data curation, writing—Original draft preparation; N.A.F. & N.M.V.: Visualization, investigation; N.M.V.: Supervision; N.A.F.: Software, validation; N.A.F. & N.M.V.: Writing—Reviewing and editing. All authors have read and agreed to the published version of the manuscript.

Funding

This research received no external funding.

Institutional Review Board Statement

Not applicable.

Informed Consent Statement

Not applicable.

Conflicts of Interest

The authors declare no conflict of interest.

Use of AI and AI-assisted Technologies

No AI tools were utilized for this paper.

References

1. Ho, K.H.; Newman, S.T. State of the art electrical discharge machining (EDM). *Int. J. Mach. Tools Manuf.* **2003**, *43*, 1287–1300.
2. Papazoglou, E.L.; Karmiris-Obratański, P.; Karkalos, N.E.; et al. Theoretical and experimental analysis of plasma radius expansion model in EDM: A comprehensive study. *Int. J. Adv. Manuf. Technol.* **2023**, *126*, 2429–2444.
3. Petropoulos, G.P.; Vaxevanidis, N.M.; Radovanovic, M.; et al. Morphological: Functional aspects of electro-discharge machined surface textures. *Stroj. Vestn.* **2009**, *55*, 95–103.
4. Petropoulos, G.; Vaxevanidis, N.M.; Pandazaras, C. Modeling of surface finish in electro-discharge machining based upon statistical multi-parameter analysis. *J. Mater. Process. Technol.* **2004**, *155*, 1247–1251.
5. Petropoulos, G.; Vaxevanidis, N.; Iakovou, A.; et al. Multi-parameter modeling of surface texture in EDMachining using the design of experiments methodology. *Mater. Sci. Forum.* **2006**, *526*, 157–162.
6. Zhang, Y.; Bai, X.-L.; Xu, X.; et al. STEP-NC Based High-level Machining Simulations Integrated with CAD/CAPP/CAM. *Int. J. Autom. Com.* **2012**, *9*, 506–517. <https://doi.org/10.1007/s11633-012-0674-9>.
7. De Silva, A.K.M.; McGeough, J.A. Computer applications in unconventional machining. *J. Mater. Process. Technol.* **2000**, *107*, 276–282.
8. Vikas, R.A.K.; Kumar, K. Effect and Optimization of Machine Process Parameters on Material Removal Rate in EDM for EN41 Material Using Taguchi. *Int. J. Mech. En. Computer Appl.* **2013**, *1*, 35–39.
9. Younis, M.A.; Abbas, M.S.; Gouda, M.A.; et al. Effect of electrode material on electrical discharge machining of tool steel surface. *Ain Shams Eng. J.* **2015**, *6*, 977–986. <https://doi.org/10.1016/j.asej.2015.02.001>.
10. Raghuraman, S.; Thirupathi, K.; Panneerselvam, T.; et al. Optimization of EDM parameters using taguchi method and grey relational analysis for mild steel IS 2026. *Int. J. Innovative Res. Sci. Eng. Technol.* **2013**, *2*, 3095–3104.
11. Markopoulos, A.P.; Manolakos, D.E.; Vaxevanidis, N.M. Artificial neural network models for the prediction of surface roughness in electrical discharge machining. *J. Intell. Manuf.* **2008**, *19*, 283–292.
12. Markopoulos, A.P.; Papazoglou, E.L.; Svarnias, P.; et al. An experimental investigation of machining aluminum alloy Al5052 with EDM. *Proc. Manuf.* **2019**, *41*, 787–794.
13. Markopoulos, A.P.; Papazoglou, E.L.; Karmiris-Obratański, P. Experimental study on the influence of machining conditions on the quality of electrical discharge machined surfaces of aluminum alloy Al5052. *Machines* **2020**, *8*, 12.

14. Balanou, M.; Karmiris-Obratański, P.; Karkalos, N.E.; et al. On the Machining of Aluminum Alloy Series 7 with EDM. In *International Scientific-Technical Conference Manufacturing*; Springer International Publishing: Cham, Switzerland, 2022; pp. 149–160.
15. Cavaleri, L.; Chatzarakis, G.E.; Di Trapani, F.; et al. Modeling of surface roughness in electro-discharge machining using artificial neural networks. *Adv. Mater. Res.* **2017**, *6*, 169–184.
16. Mishra, S.S.; Mahapatra, K.; Mahapatra, K.K.; et al. Advancement in the EDM Process: A Critical Review. In *Current Advances in Mechanical Engineering. Lecture Notes in Mechanical Engineering*; Acharya, S.K., Mishra, D.P., Eds.; Springer: Singapore, 2021. https://doi.org/10.1007/978-981-33-4795-3_77.
17. Asteris, P.G. Computational Intelligence: From Nature and Aristotle to Meta-Heuristic Algorithms. *Bull. Comput. Intell.* **2025**, *1*, 1–2. <https://doi.org/10.53941/bci.2025.100001>.
18. Mirjalili, S. Moth-flame optimization algorithm: A novel nature-inspired heuristic paradigm. *Knowl.-Based Sys.* **2015**, *89*, 228–249. <https://doi.org/10.1016/j.knosys.2015.07.006>.
19. Mirjalili, S. Dragonfly algorithm: A new meta-heuristic optimization technique for solving single-objective, discrete, and multi-objective problems. *Neural Comput. Appl.* **2016**, *27*, 1053–1073. <https://doi.org/10.1007/s00521-015-1920-1>.
20. Mirjalili, S.; Lewis, A. The Whale Optimization Algorithm. *Adv. Eng. Soft.* **2016**, *95*, 51–67. <https://doi.org/10.1016/j.advengsoft.2016.01.008>.
21. Yang, X.-S.; Karamanoglu, M. Swarm Intelligence and Bio-Inspired Computation: An Overview. In *Swarm Intelligence and Bio-Inspired Computation*; Yang, X.-S., Cui, Z., Xiao, R., et al., Eds.; Elsevier: Amsterdam, The Netherlands, 2013; pp. 3–23, ISBN 9780124051638. <https://doi.org/10.1016/B978-0-12-405163-8.00001-6>.
22. Tran, V.T.; Le, M.H.; Vo, M.T.; et al. Optimization design for die-sinking EDM process parameters employing effective intelligent method. *Cogent Eng.* **2023**, *10*, 2264060. <https://doi.org/10.1080/23311916.2023.2264060>.
23. Ranajit, M.; Das, M. Sustainable EDM production of micro-textured die-surfaces: Modeling and optimizing the process using machine learning techniques. *Measurement* **2025**, *242*, 115775. <https://doi.org/10.1016/j.measurement.2024.115775>.
24. Alkayem, N.F.; Parida, B.; Pal, S. Optimization of friction stir welding process using NSGA-II and DEMO. *Neural Comput. Appl.* **2019**, *31*, 947–956. <https://doi.org/10.1007/s00521-017-3059-8>.
25. Alkayem, N.F.; Parida, B.; Pal, S. Optimization of friction stir welding process parameters using soft computing techniques. *Soft Comput.* **2017**, *21*, 7083–7098. <https://doi.org/10.1007/s00500-016-2251-6>.